Progress In Electromagnetics Research C, Vol. 137, 223–233, 2023

Study on Ultrasonic Propagation Characteristics of Partial Discharge in 10 kV XLPE Cable

Xiaohe Zhao[1, 2, *], Liujie Wan[1, 2], Jie Yang[1, 2], Shiqiang Li[3], and Wenxiang Shang[1]

Abstract—In XLPE cables, partial discharge (PD) is often accompanied by the generation of ultrasound waves, which can be used to estimate the location and size of PD. Studying the propagation law of ultrasound along the cable is of great significance for establishing the mathematical model of PD and the layout method of ultrasonic detection terminal. This article adopted simulation and experiment to study the propagation law of PD ultrasound in cables. The results indicated that the propagation process of ultrasonic waves can be divided into three stages when ultrasonic waves propagate along the cables: the diffusion process with the characteristics of spherical waves, the propagation process which is rather similar to plane waves, and the transition process of both. When the ultrasonic waves propagate along the cable, the ultrasonic amplitude attenuates and exhibits multi-peak characteristics as the distance increases. By analyzing the signal strength of the experimental results, it was found that the ultrasonic amplitude decays exponentially with propagation distance due to viscous heat loss of materials and the air gaps between cable layers, which provided a reference to the placement of distributed ultrasonic terminal for insulation weakness and design of spatial localization algorithm for PD.

1. INTRODUCTION

Crosslinked Polyethylene (XLPE) power cables are widely used in urban power supply networks [1]. Partial discharge (PD) in cables accelerates the aging of insulation materials and affects their electrical performance. The detection of partial discharge is the main means of online monitoring of the working status of cable power lines [2, 3]. It is generally believed that the acoustic wave is generated at the same time when PD occurs as [4, 5]. The ultrasonic method has no direct electrical connection to the cable line and has good electromagnetic interference resistance [6, 7]. It can achieve distributed and quasi-distributed detection, which has attracted much attention in recent years.

Rohwetter et al. employed a single mode optical fiber Sagnac ultrasonic sensor to study the PD process of silicone rubber in cable joints under AC and DC voltage [8]. A DC PD pulse about 100 pC was simultaneously measured above the positive polarity DC partial discharge inception voltage (PDIV), verifying the performance of the Sagnac optical fiber sensing system in detecting typical defects in cable joints. They used a quasi-distributed optical fiber ultrasonic detection system based on Rayleigh reflection coherent optical time domain interference to detect PD defects in 40 kV XLPE cable joints and detected nC level discharge signals, which proved for the first time that this quasi-distributed optical fiber acoustic sensing technology is a candidate technology for ultrasonic monitoring of PD in power cable joints and terminals [9]. Czaszejko and Stephens were able to detect the internal discharge of 10 pC by detecting the PD ultrasonic signals inside and along the surface of the XLPE sample using a Bragg fiber grating sensor. In cables, the magnitude of PD, the location of the discharge

Received 21 June 2023, Accepted 2 September 2023, Scheduled 13 September 2023
* Corresponding author: Xiaohe Zhao (15893860381@163.com).
[1] Henan Institute of Technology, Xinxiang 453000, Henan, China. [2] Henan Key Laboratory of Cable Structure and Materials, Xinxiang 453000, Henan, China. [3] Institute of Electrical Engineering, Chinese Academy of Sciences, Beijing 100190, China.

source, and the type of discharge defects are crucial to the diagnosis of PD defects [10]. Wang et al. fabricated four types of defects in the XLPE cable intermediate joint, including internal air gap, burr, sliding flash, and suspended discharge. Using piezoelectric ceramic ultrasonic sensors, they obtained the PD ultrasonic signal waveforms of these four types of defects and discussed the time and frequency domain characteristics of the waveforms [11]. Li et al. studied the time domain and phase spectrum characteristics of PD ultrasonic signals from three types of defects on XLPE materials: tip discharge, air gap discharge, and surface discharge in a laboratory environment, and studied the relationship between different voltages and maximum discharge amplitude, average discharge amplitude, and discharge times [12]. Wang et al. studied the acoustic detection method in power cable and established a PD analysis model that integrates ultrasonic and electromagnetic methods [13].

XPLE cables are composed of multi-layer insulating materials with complex structures. The sound velocity and acoustic impedance of each layer of material are different which makes the propagation process of sound waves more complex than in a uniform medium, and at the same time, the viscous heat loss of insulation materials and the small air gaps in cable structure can also cause attenuation of acoustic energy amplitude [14, 15]. However, the existing research on the propagation law of ultrasonic signals in XPLE cables is relatively incomplete, lacking measured results and clear models for cables, which makes it difficult to obtain accurate PD information from the ultrasonic signals of detection terminals.

In order to study the propagation process of ultrasonic waves in cables, this paper established a sound pressure field simulation model for 10 kV XLPE cable body without neglecting the material absorption attenuation and viscous loss, and studied the propagation process of ultrasonic waves in cables from the sound source point in detail. By setting process defect discharge points at the intermediate joints of cables, the propagation law and detection signal characteristics of PD ultrasonic signals along the cables at different locations were experimentally studied.

2. ATTENUATION MECHANISM OF ULTRASONIC WAVES IN CABLES

The structural diagram of a 10 kV XLPE single conductor cable studied in this paper is shown in Fig. 1, which consists of aluminum stranded conductor and multiple layers of dielectric. The material parameters of each layer are as shown in Table 1. When there are defects such as bubbles or foreign particles in the insulator or spikes in the semiconductive layer surfaces of the insulation screen and conductor screen, PD is prone to occur at these weak points, and the ultrasonic signals generated will also propagate from these positions to other parts of the cable.

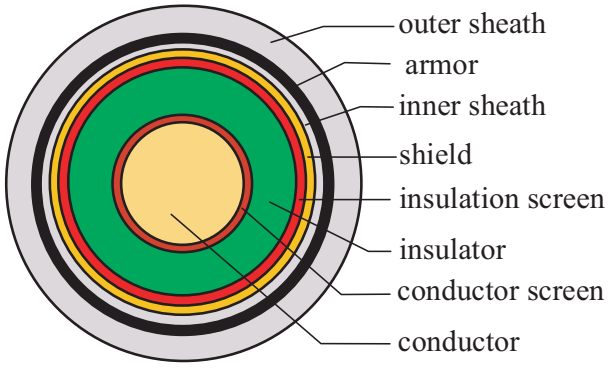

Figure 1. Sectional structure diagram of a 10 kV XLPE cable.

According to the acoustic wave equation in solids.

$$\rho\frac{\partial^2\mathbf{v}}{\partial t^2} = (\lambda+2\mu)\,\nabla(\nabla\cdot\mathbf{v}) - \mu\nabla\times(\nabla\times\mathbf{v}) \tag{1}$$

where ρ is the mass density of the material; $\mathbf{v}$ is the particle vibration velocity; ∇ is a Hamilton operator, which is $\nabla = \frac{\partial}{\partial x}\mathbf{e}_x + \frac{\partial}{\partial y}\mathbf{e}_y + \frac{\partial}{\partial y}\mathbf{e}_y$ in Cartesian coordinates; λ and μ are the Lame coefficient of solid

Table 1. Acoustic parameters of each layer structure of 10 kV XLPE cable.

structure	thickness /mm	density /gm^{-3}	sound velocity /ms^{-1}	Young's modulus /GPa	Poisson's ratio	acoustic impedance /10^6 Ns $\cdot$ m^{-3}
Aluminum core	R4.75	2700	625	0.7	0.3	16.875
XLPE insulator	5	930	2160	0.9	0.38	2.418
Insulation screen	1.5	150	2100	0.11	0.33	2.205
Conductor screen	1	1050	2100	0.11	0.33	2.205
Copper shield	0.05	8960	381	110	0.35	32.776
Steel-tape armor	0.2	7930	5800	195	0.247	45.994
Outer sheath	3	2230	2400	0.3	0.38	5.35
inner sheath	1	2230	2400	0.3	0.38	5.35

material, which satisfy the following relationship with the Young's modulus and Poisson's ratio of the material.

$$\lambda = \frac{E\sigma}{(1+\sigma)(1-2\sigma)} \quad \mu = \frac{E}{2(1+\sigma)} \tag{2}$$

According to Helmholtz theorem, vector fields can be expressed as the sum of scalar gradients and vector curls. Assume

$$\begin{cases} \mathbf{v} = \nabla\Phi + \nabla \times \mathbf{\Psi} \\ \nabla \cdot \mathbf{\Psi} = 0 \end{cases} \tag{3}$$

where Φ and Ψ are scalar potential and vector potential, respectively.

Substitute Eq. (3) into Eq. (1) and separate the variables to obtain the potential function equation of the acoustic field in solid.

$$\begin{cases} \rho\dfrac{\partial^2\Phi}{\partial t^2} = (\lambda + 2\mu)\nabla^2\Phi \\ \rho\dfrac{\partial^2\Psi}{\partial t^2} = \mu\nabla^2\Psi \end{cases} \tag{4}$$

According to Eq. (4), there are two different forms of vibration of sound waves in solids. Φ is described as a longitudinal wave with propagation velocity $c_L = \sqrt{\frac{\lambda+2\mu}{\rho}}$ and Ψ described as a transverse wave with propagation velocity $c_T = \sqrt{\frac{\mu}{\rho}}$. At the same time, sound waves also form Rayleigh waves propagating along the surface of a solid.

The local emission sound source belongs to a point shaped pulse or oscillating sound source, and the wave front of the point sound source is a spherical wave. Therefore, diffusion should be considered in the study of the propagation theory of local emission ultrasonic in cables. At the same time, ultrasonic waves are almost completely reflected at the air interface of the outer sheath, because the acoustic impedance of the outer sheath of the cable (5.35×10^6 N $\cdot$ s $\cdot$ m^{-3}) is much larger than the air acoustic impedance (0.0004×10^6 N $\cdot$ s $\cdot$ m^{-3}). The cable structure will limit the diffusion of PD ultrasonic waves, which only propagates within the cable. Therefore, it is believed that the PD ultrasound in the cable propagates longitudinally along the cable, ignoring the diffusion and attenuation of the acoustic wave [15].

In XLPE cables, due to the thin thickness of the two semi-conductive screen layers and because the acoustic characteristics are similar to those of the insulation layer, the insulation screen and conductor screen can be incorporated into insulator layer in acoustic analysis. The thickness of metal shield and metal armor layers is much smaller than that of sound waves generated by PD, and the sound impedance is much greater than the adjacent insulation material. Reflection will occur at the interface between the two media during the propagation of acoustic waves along the cable. According to Snell's law, the

incidence angle θ_i, reflection angle θ_r, and refraction angle θ_t satisfy Eq. (5).

$$\begin{cases} \theta_i = \theta_r \\ \dfrac{\sin\theta_i}{\sin\theta_t} = \frac{c_1}{c_2} \end{cases} \tag{5}$$

where c_1 and c_2 are the propagation velocity of sound waves in medium 1 and medium 2, respectively.

According to the structural characteristics of the cable, when ultrasonic wave generated by PD propagates along the cable, the direction of the acoustic wave is almost parallel to the interface of different materials, and the propagation characteristics are more consistent with the characteristics of grazing incidence acoustic waves. Therefore, interface attenuation can be ignored, and it is believed that the attenuation of ultrasound mainly consists of absorption attenuation, scattering attenuation, and diffusion attenuation. Among them, absorption attenuation is related to material properties. In cables, the absorption attenuation coefficient of XLPE for sound waves is greater than that of metal conductors and has the characteristic of frequency dispersion, that is, the high-frequency components of sound waves attenuate faster when they propagate through insulation layer. The actual cable structure consists of multi-layer composite media, with acoustic impedance differences between different media. At the same time, there are inevitably air gaps or bubbles in some components of the cable, such as small air gaps in the spiral wound steel armor layer or small bubbles in insulation materials, which can also lead to ultrasonic scattering.

It is generally believed that the attenuation of planar ultrasonic amplitude with propagation distance can be expressed by an exponential law and the exponential attenuation coefficient α (unit is: dB/mm or Np/mm, 1 Np/mm = 8.686 dB/mm), including scattering attenuation coefficient α_s and absorption attenuation coefficient α_a.

$$\alpha{=}\alpha_s + \alpha_a \tag{6}$$

where $\alpha_a = C_1 f$,

$$\alpha_s = \begin{cases} C_2 F d^2 f^4, d \ll \lambda \\ C_3 F d f^2, d \approx \lambda \\ C_4 F d^{-1}, d \gg \lambda \end{cases} \tag{7}$$

where C_1, C_2, C_3, and C_4 are constants; F is an anisotropic coefficient; d is the grain diameter; λ is the ultrasonic wavelength; f is the ultrasonic frequency.

According to the above analysis, the propagation process of ultrasound along the cable is a complex model involving multiple media. This paper adopts a combination of finite simulation analysis and experimental methods to study the general propagation laws of the ultrasound generated by PD.

3. SIMULATION ANALYSIS OF ATTENUATION LAW OF ACOUSTIC WAVE AMPLITUDE IN CABLE

3.1. Simulation Model

According to the generation mechanism of PD ultrasonic signals, a single pole point acoustic source is employed to simulate the PD ultrasonic source, and the propagation process of ultrasonic along the cable is studied.

A 3-D simulation model in COMSOL Multiphysics was constructed according to the structural parameters of a certain model cable of YJLV series. The rated voltage of the studied cable is 10 kV, with aluminum core and cross-linked polyethylene (XLPE) insulator. The material parameters of each structure are shown in Table 1.

Due to the small difference in acoustic properties of semiconductive layer materials, the inner and outer semiconductive layers are combined with insulator to simplify the calculation model. At the same time, the thicknesses of the steel armor layer and copper shield layer are 0.2 mm and 0.05 mm, respectively, which are much smaller than the ultrasonic wavelength. To simplify the model and improve the calculation efficiency, the steel armor layer and copper shield layer are merged into insulation layer and equivalent to a shell structure whose parameters and dimensions are consistent with the actual

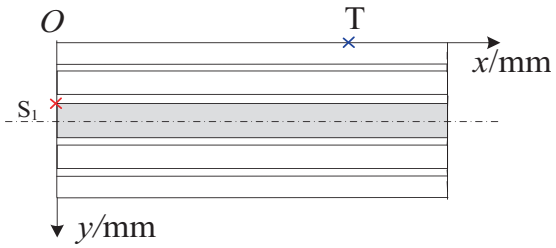

Figure 2. Model of cable sound pressure field simulation.

structure. The axial length of the model is set to 2 m. The longitudinal section of the simulation model is shown in Fig. 2.

Due to the small spatial scale of PD in the cable, most of the sound sources have the characteristics of point source. The typical locations of PD include the outer surface of metal conductor, the impurities inside the insulation, and the outer surface of insulation layer, shown as S_1, S_2, and S_3 respectively in Fig. 2.

A Gaussian volume flow rate is employed to simulate the sound source generate by PD, and the expression is as follows.

$$Q_s = A \cdot \exp\left[-\pi^2 \cdot f_0^2 \cdot (t - t_p)^2\right] \tag{8}$$

where Q_s is the volume flow rate, whose unit is m^3/s; A is the initial value of the volumetric flow rate; t_p is the pulse peak time; and f_0 is the center frequency of the pulse. According to the research object of this question, take $A = 1\,m^3/s$, $t_p = 10\,\mu s$, $f_o = 20\,kHz$. The waveform and spectrum diagram of pulsed sound are shown in Fig. 3.

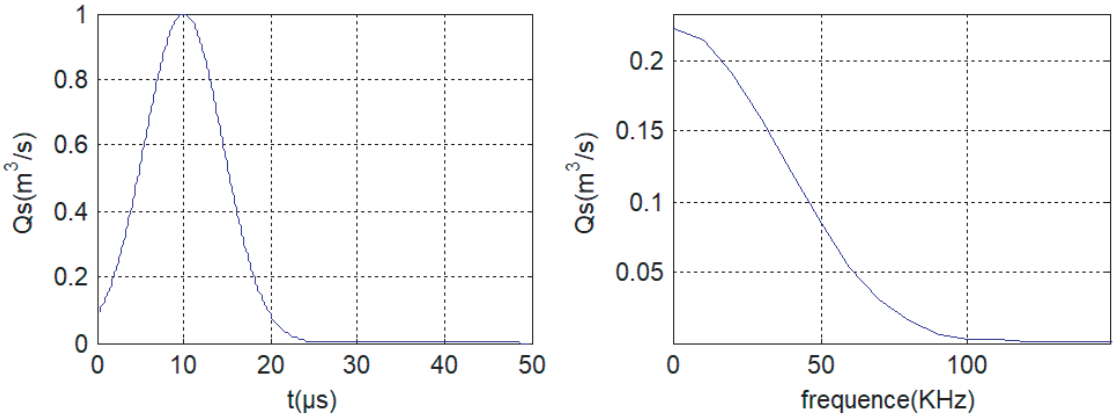

Figure 3. Waveform of Gauss pulse.

3.2. Simulation Results and Analysis

The sound waves inside the cable will undergo a diffusion process starting from the source point, and the development of the diffusion process can be reflected as the changes in the wavefront shape. As shown in Fig. 4, in the initial stage of sound wave propagation, the wavefront is closer to a spherical wave, and as the sound wave propagates along the cable, the wavefront shape gradually transforms to a plane. When the propagation distance of sound waves along the cable is greater than 110 mm, ultrasonic waves have the characteristics of plane waves.

The propagation changing process of sound waves can also be explained by the changes of wavefront shape. The right part of Fig. 4 shows the distribution of the acoustic pressure field on the cable section at 20 μs, 40 μs, and 60 μs, respectively. It can be seen that the ultrasonic wave front inside the cable

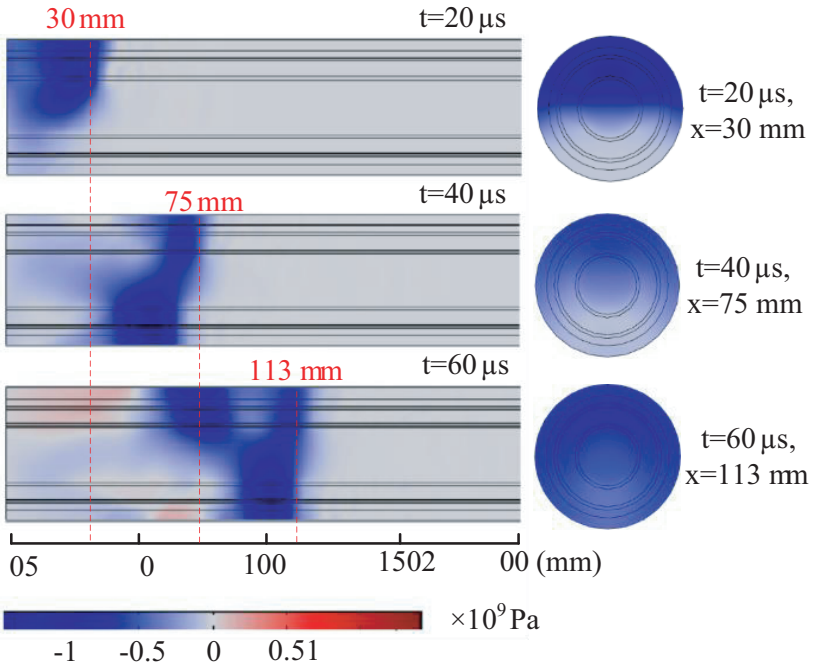

Figure 4. Distribution of sound field in cable section of $Z = 0$ in different time.

moves forward with time, and the shape of the wave front gradually changes from a curved surface to a plane.

In practical testing, ultrasonic sensors are generally installed on the surface of the outer sheath of the cable. According to the coordinate system shown in Fig. 2, sound pressure detection points T_i $(i = 1, 2, \ldots, 19)$ are set at different distances along the axial direction on the surface of the outer sheath on the model. The y-axis and z-axis coordinates of the detection points are both zero, and their x coordinates are as shown in Table 2.

Table 2. x coordinate of detection points of acoustic pressure.

detection points	T_1	T_2	T_3	T_4	T_5	T_6	T_7	T_8	T_9	T_{10}
x/mm	10	20	30	40	50	60	70	80	90	100
detection points	T_{11}	T_{12}	T_{13}	T_{14}	T_{15}	T_{16}	T_{17}	T_{18}	T_{19}	
x/mm	200	300	400	500	600	700	800	900	1000	-

Sound pressure time responses at points T_2, T_6, T_{10}, and T_{11} are extracted as shown in Fig. 5. According to Fig. 5, points T_2 and T_6 correspond to the diffusion zone and transition zone, respectively, and T_{10} and T_{11} are both in the plane wave propagation zone. It can be seen that the amplitude of sound pressure gradually decreases as the propagation distance increases, and gradually exhibits a multi-peak characteristic, which is caused by the reflection and refraction of sound waves as they propagate through the cable due to the differences in acoustic characteristics of different structural materials of the cable. During the plane waves propagation, the characteristics of waveform gradually become stable, and the amplitude of the waveform decreases with the propagation distance.

The simulation results indicate that during the diffusion stage of ultrasonic signals, the wavefront does not exhibit axisymmetric characteristics, and the detection signal on the outer surface of the cable is related to the circumferential position. Considering the randomness of PD positions, signal receiving terminals should be installed in the plane wave propagation range in practical applications.

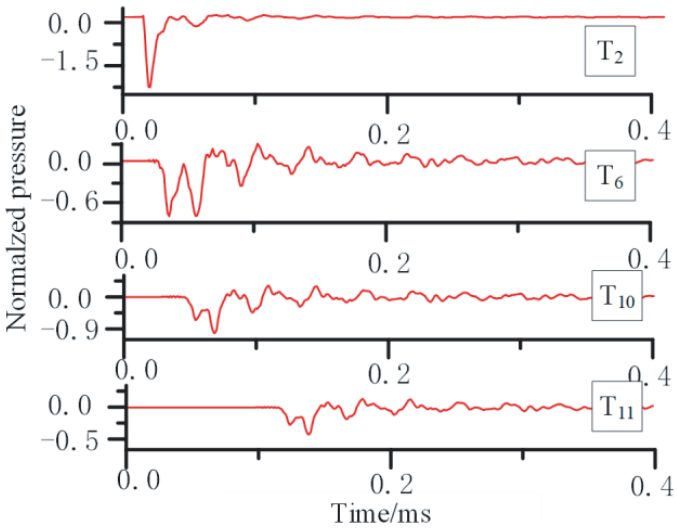

Figure 5. Sound pressure-time curve of detection point T_2, T_6,T_{10} and T_{11}.

4. EXPERIMENT AND ANALYSIS OF PD SOUND WAVE IN CABLE

A PD ultrasonic detection platform for a certain type of 10 kV single-phase cable has been built, and the experimental system diagram is shown in Fig. 6.

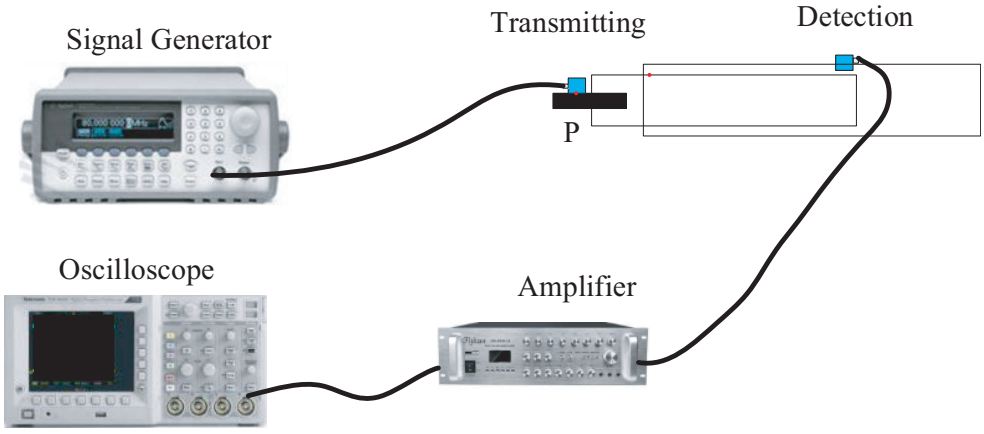

Figure 6. Experimental system diagram.

The signal generator outputs a voltage waveform consistent with the characteristics of the PD sound and drives the transmitting transducer, which was placed on point P to simulate the ultrasonic signal produced by PD occurring on the conductor surface. The detection transducer receives sound pressure signals at different positions along the cable. Then, the signals are adjusted by an amplifier and collected by an oscilloscope. Based on this experimental platform, two studies were conducted: installation method for acoustic signal receiving terminals and attenuation law of sound waves along the cable.

The length of the experimental cable is 5 meters. The sheath and insulation structure at one end are removed to expose the conductor. The transmitting transducer injects sound waves into the outer surface of the conductor through an epoxy resin coupling block, while the receiving transducer is attached to the outer surface of the cable through a coupling block. The axial distance between two transducers is denoted as x.

4.1. Research of Installation Method for Detection Terminals

In order to study the effect of the angle between the detection transducer and the sound source position, a plane with axial detection distance of $x = 200$ mm was selected, as shown in Fig. 7(a). Four sensors at different positions were installed on the plane, with angles of 0°, 90°, 180°, and 270° with sound source, respectively. The radial position of the PD source and the detection transducers are as shown in Fig. 7(b).

The detection waveforms are as shown in Fig. 8. It indicates that on the same detection plane, the acoustic signals at different positions are basically identical, which is consistent with the simulation

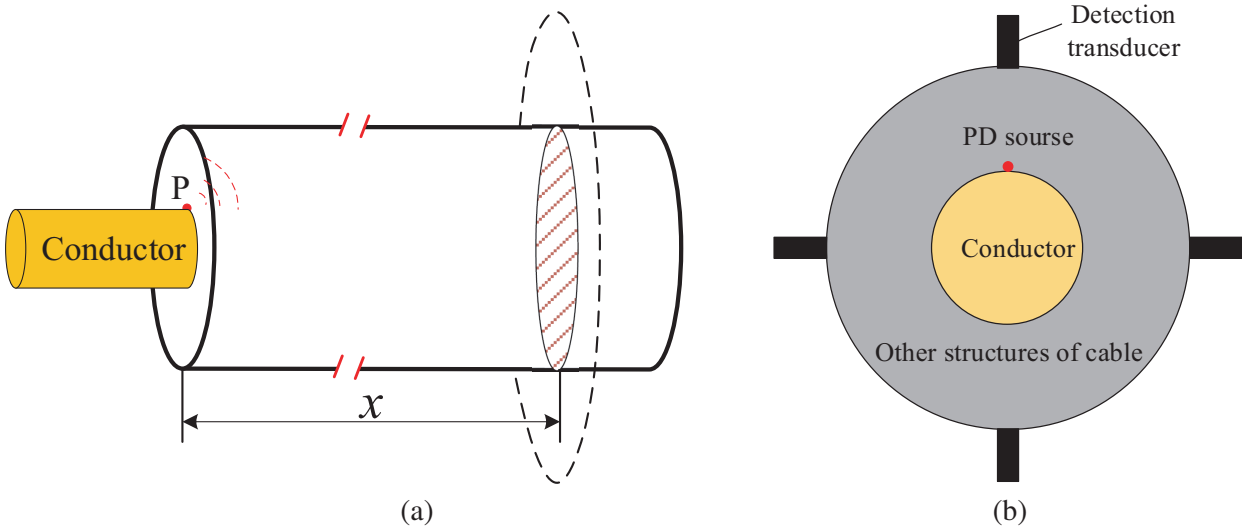

Figure 7. Detection scheme for different circumferential positions. (a) Schematic diagram of detection plan. (b) The installation position of sensors in the detection plane.

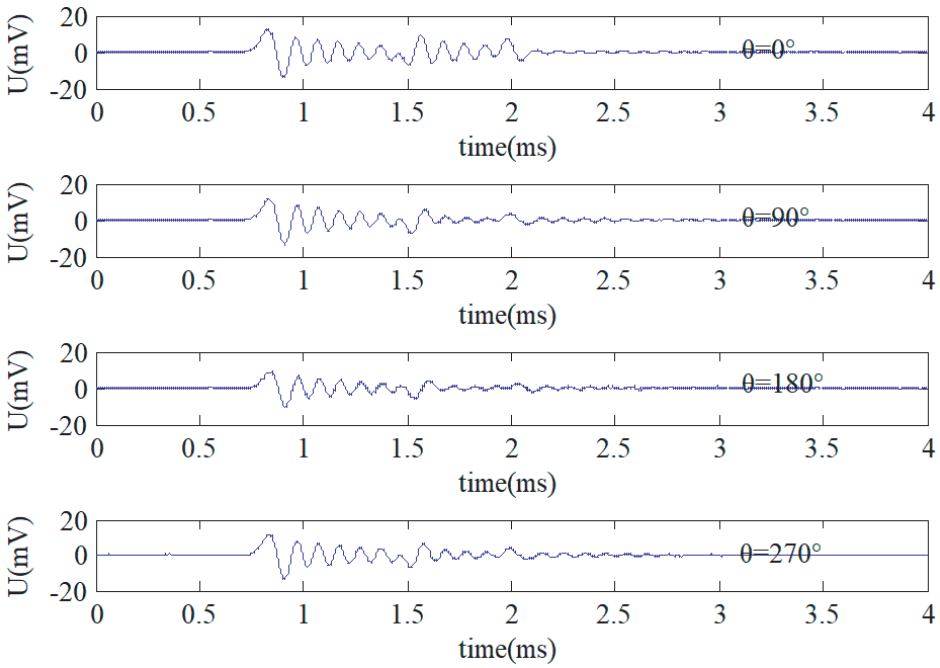

Figure 8. Waveform detection at different positions.

results. It is verified that sound waves have the characteristics of plane waves when propagating over long distance along cable lines.

4.2. Attenuation Law of Sound Waves Along Cable

The axial coordinates of each detection point are shown in Table 2. The sound pressure signals at different detection positions are as shown in Fig. 9. It can be seen that there is significant difference in signal amplitude and waveform as the propagation distance increases. First of all, the detection signal gradually exhibits the characteristics of multiple clusters of signals, which is consistent with the trend

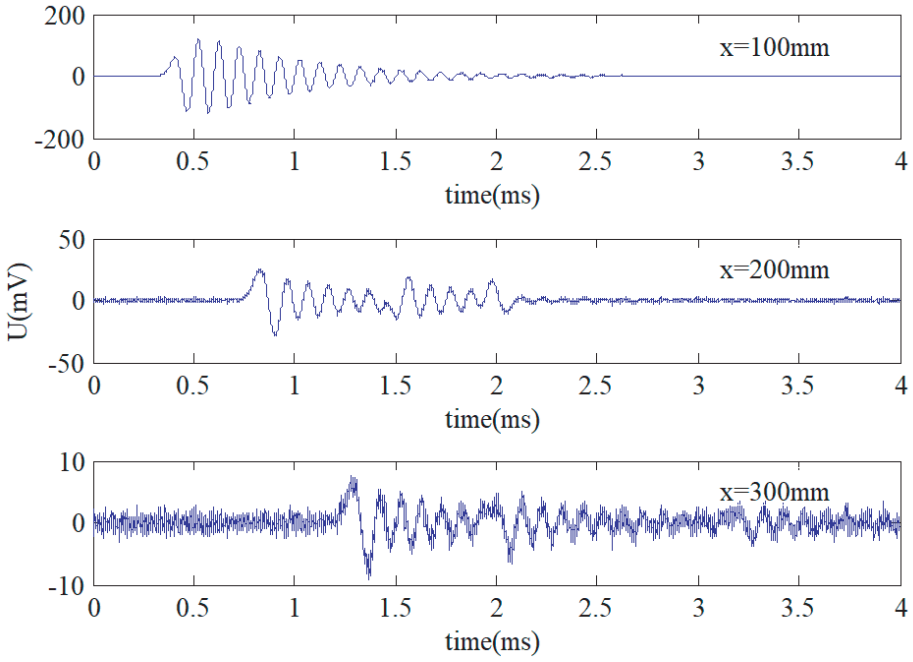

Figure 9. Sound pressure at different positions.

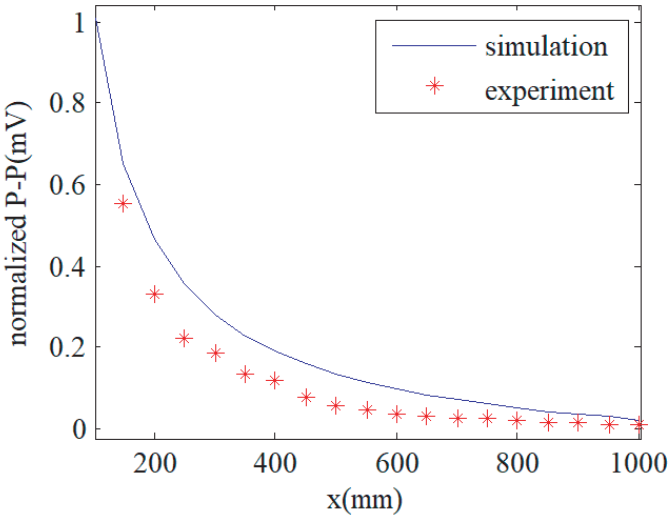

Figure 10. Attenuation law of sound pressure signal.

of multi-peak changes in the sound pressure signal in simulation. At the same time, sound pressure amplitude decreases rapidly as the propagation distance increases.

The P-P values of multiple detection point waveforms along the cable were extracted, and the attenuation law of ultrasonic signal intensity along the cable was studied. The result was as shown in Fig. 10, which indicates that the attenuation of measured signal is faster than that of the simulation. This is due to the small-sized air gaps at the interface between two materials of the cable, which hinders the radial propagation of acoustic vibration energy. At the same time, poor coupling between the sensor and the outer surface of the cable can also weaken the measurement signal strength.

In the experiment, increasing the contact pressure between the ultrasonic sensor and the outer surface of the cable can effectively enhance the amplitude of the detection signal. As shown in Fig. 11, the amplitude of the detection signal is nearly doubled when 10 N pressure is added to the detection sensor.

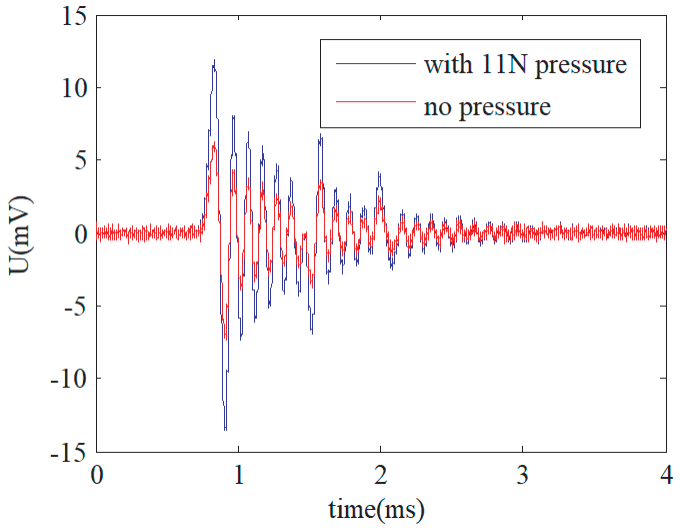

Figure 11. Signals of sensors with different installation pressures.

5. DISCUSSION AND CONCLUSION

This article employed simulation and experimental methods to study the propagation law of ultrasonic signals generated by PD in cables. A simulation model for one type of 10 kV XLPE cable was established. The internal propagation process of PD ultrasonic cable was studied, and the ultrasonic attenuation in the 10 kV single-phase XLPE cable was measured on the cable ultrasonic attenuation experimental system. The results indicate that:

(1) The ultrasonic waves generated by PD in cables are greatly affected by the acoustic properties differences of the materials in each layer of the cable during propagation along the cable. In longitudinal propagation, sound waves are separated due to the velocity difference of sound in each layer. By utilizing the differences in sound velocity among various materials, the accurate localization of PD can be achieved, which provides new ideas for precise localization methods of PD.

(2) In the longitudinal propagation of sound waves along cables, the amplitude attenuation is equivalently fast. During the propagation of sound waves along the cable, the amplitude attenuation of sound waves along the cable is fast, and the propagation distance is small, which makes the ultrasonic method unable to be used for remote PD signal detection. Both simulated and experimental results indicate that the detection range of PD signals using ultrasonic method do not exceed 500 mm, which is more suitable for distributed ultrasonic testing near the cable intermediate joint.

The research results of this paper provide a basis for building a distributed information detection system for key parts of cables using ultrasonic testing method.

ACKNOWLEDGMENT

This research was supported by Henan Science and Technology Projects Fund in 2022 (No. 222102220102)) and Henan Key Laboratory of Cable Structure and Materials, Henan Institute of Technology (No. HKL-CSM2022002).

REFERENCES

1. Tian, Y., P. L. Lewin, A. E. Davies, et al., "Acoustic emission detection of Partial Discharges in polymeric insulation," *1999 Eleventh International Symposium on High Voltage Engineering*, Vol. 1, 82–85, London, UK, 1999.
2. Nie, Y., X. Zhao, and S. Li, "Research progress in condition monitoring and insulation diagnosis of XLPE cable," *High Voltage Engineering*, Vol. 46, No. 04, 1361–1371, 2020.
3. Chen, Y., Y. Hao, T. Huang, et al., "Voltage equivalence of partial discharge tests for XLPE insulation defects," *IEEE Transactions on Dielectrics and Electrical Insulation*, Vol. 29, No. 2, 683–692, April 2022.
4. Nakanishi, Y., Y. Nakatani, M. Iizumi, et al., "Partial dis-charge detection by AE sensors for prefabricated joints for XLPE cables," *Electrical Engineering in Japan*, Vol. 113, No. 8, 73–83, 1993.
5. Czaszejko, T. and J. Sookun, "Acoustic emission from partial discharges in cable termination," *ISEIM*, 2014.
6. Hsieh, J.-C., C.-C. Tai, C.-C. Su, et al., "The transmission characteristics of sound wave in power cable," *2008 International Conference on Condition Monitoring and Diagnosis*, 1228–1231, Beijing, 2008.
7. Robles, G., M. Shafiq, and J. M. Martinez-Tarifa, "Multiple partial discharge source localization in power cables through power spectral separation and time-domain reflectometry," *IEEE Transactions on Instrumentation and Measurement*, 1–9, 2019.
8. Rohwetter, P., R. Eisermann, and K. Krebber, "Distributed acoustic sensing: Towards partial discharge monitoring," *24th International Conference on Optical Fiber Sensors*, 96341C, 2015.
9. Rohwetter, P. and W. Habel, "Acoustic emission from DC pre-treeing discharge processes in silicone elastomer," *IEEE Transactions on Dielectrics and Electrical Insulation*, Vol. 22, No. 1, 2015.
10. Czaszejko, T. and A. D. Stephens, "Toward acoustic detection of partial discharges in high voltage cables," *9th International Conference on Insulated Power Cables. Versailles: Jicable'15*, E8.2, 2015.
11. Wang, W., X. Cheng, and C. Liu, "Study on the frequency spectrums of acoustic emission PD signals in XLPE cable accessories," *2008 International Conference on Condition Monitoring and Diagnosis*, 1246–1249, Beijing, 2008.
12. Li, J., W. Cao, R. Liu, et al., "Measurement and analysis of partial discharge in XLPE power cable based on ultrasonic," *Journal of Shaanxi Normal University (Natural Science Edition)*, Vol. 45, No. 6, 29–37, 2017.
13. Wang, Y., L. Xiong, H. Tang, and Z. Zhang, "Acoustic detection and decision fusion recognition of PD in power cable," *2021 IEEE 2nd China International Youth Conference on Electrical Engineering*, 1193–1198, IEEE, 2021.
14. Ilkhechi, H. D. and M. H. Samimi, "Applications of the acoustic method in partial discharge measurement: A review," *IEEE Transactions on Dielectrics and Electrical Insulation*, Vol. 28, No. 1, 42–51, 2021.
15. Hsieh, J., C. Tai, C. Su, C. Chen, J. Chen, et al., "The application of partial discharge detector and electro-acoustic signals analysis methods for power cables monitoring," *2012 IEEE International Conference on Condition Monitoring and Diagnosis*, 157–160, Bali, 2012.